

# Hydrogel-based standards for single and multiphoton imaging at depth

Fizza Haseeb<sup>a</sup>, Konstantinos N. Bourdakos<sup>d</sup>, Ewan Forsyth<sup>a</sup>, Kerry Setchfield<sup>c</sup>, Alistair Gorman<sup>b</sup>,  
Seshasailam Venkateswaran<sup>e</sup>, Amanda J. Wright<sup>c</sup>, Sumeet Mahajan<sup>d</sup>, Mark Bradley<sup>\*e</sup>

<sup>a</sup>School of Chemistry, University of Edinburgh, David Brewster Road, EH9 3FJ Edinburgh; <sup>b</sup>School of Engineering, University of Edinburgh, Alexander Crum Brown Road, Edinburgh EH9 3FF;

<sup>c</sup>Optics and Photonics Research Group, Faculty of Engineering, University of Nottingham,

Nottingham, NG7 2RD; <sup>d</sup>School of Chemistry, Faculty of Engineering and Physical Sciences,

University of Southampton, SO17 1BJ Southampton, UK; <sup>e</sup>Precision Healthcare University Research Institute, Queen Mary University of London, Whitechapel, Empire House, London E1 1HH, UK

## ABSTRACT

Medical imaging is advancing rapidly through the development of novel laser sources and non-linear imaging methodologies. These developments are boosting deep tissue imaging allowing researchers to study diseases deep in the body enabling early diagnosis and better treatment. To help with the testing and optimization of these imaging systems and to aid in this process of deep tissue imaging, it's important to have robust, stable and reproducible standards and phantoms. Herein we present the design and fabrication of robust, multi-layered, hydrogel-based standards. The hydrogel used is a double network hydrogel consisting of two interpenetrating networks agarose and polyacrylamide. Thin layers of tough double network hydrogels are stacked to form multilayered depth standards having modality specific signaling markers embedded in between. Standard design and assembly ensured long term stability and easy transport. These proved useful in-depth imaging studies, utilizing multiple imaging modalities, including one photon fluorescence (1PEF), two photon fluorescence (2PEF), coherent anti-Stokes Raman imaging (CARS) and second harmonic generation imaging (SHG).

**Keywords:** Depth imaging, multiphoton imaging, standards, phantoms, fluorescence, raman, double network, hydrogel

\* Mark Bradley, E-mail: m.bradley@qmul.ac.uk

## 1. INTRODUCTION

The era of molecular medicine has been a catalyst for remarkable advancements in microscopic technologies. These microscopic techniques allow reporting of molecular processes in tissues with high spatial resolution. Microscopic examination of thick tissue sections, typically exceeding 0.5 mm, as well as live animal studies, requires imaging systems and modalities that have the capability to image deeper than what is required for cellular-level observations. The strategic use of near-infrared (NIR) lasers with single- or multiphoton excitations can allow deep tissue imaging. Sarder et al demonstrated this by imaging mice kidney *ex vivo*. By utilizing single and multiphoton NIR imaging systems, he found imaging depth to be 5 times greater in NIR (excitation and emission) multiphoton system than Single Photon NIR confocal microscopy.<sup>1</sup>

Currently phantoms or standards that can help researchers monitor this slow progress in imaging depth are lacking. Standards capable of integrating specific markers or targets for single and multiphoton imaging systems are crucial for advancing deep tissue optical imaging and the development of new imaging techniques. One way to develop such standards is through the use of laser written fluorescence patterns<sup>2</sup>. This technique is used in the point spread function (PSF) check slides to generate two- and three- dimensional patterns, used for the optical characterization of fluorescence microscopes. Other ways include multilayering solid resin or hydrogel phantoms<sup>3</sup> or incorporating channels in a solid resin<sup>4</sup>. However, there is a need for standards that are versatile in terms of markers, are robust and stable and easily transportable as it would allow uniform testing and comparison across different systems.

In this paper, we demonstrate the fabrication of depth standards made using two double network hydrogel matrices agarose and polyacrylamide. The standards were built as stacks of thin layers of hydrogels (190  $\mu\text{m}$  - 2000  $\mu\text{m}$  in thickness) with signaling markers embedded in between. To protect standards from dehydration, the standards were sealed in wellplates using polydimethylsiloxane (PDMS) resin (Fig. 1). Sealed standards proved stable for months, thus reducing the barriers to their adoption across the research community. Here, the standards were tested on single and multiphoton imaging systems and proved useful for depth evaluation studies for single and multiphoton imaging systems.

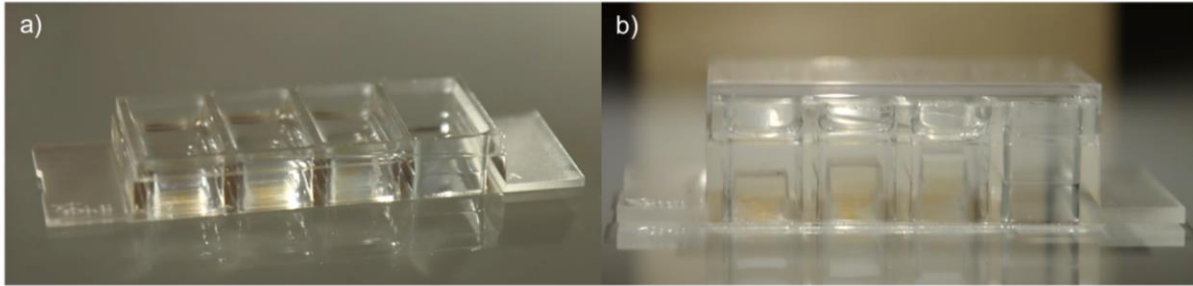


Figure 1: Images of well plates containing the depth standards. a, b) Side views of the fabricated standards. Well plate outer dimensions (w x l) 25.5 x 75.5 mm<sup>2</sup>.

## 2. METHODS

### 2.1 Synthesis of double network hydrogel:

For the preparation of double network hydrogel, Acrylamide (1.78 g), N, N'-methylene-bis-acrylamide (1.8 mL, 1% w/v in water), Irgacure 2959 (56 mg), Agarose (200 mg), and water (8.2 mL, HPLC grade) were added into a microwave glass vial (Biotage® 10 to 20 mL, Part No. 354833). The solution was flushed with nitrogen (30 min) and the vials were sealed from top. Solution was heated to a high temperature (90°C) in an oil bath until a transparent solution was obtained. To prepare gels in thin layers (thickness > 200  $\mu\text{m}$ ), two plastic spacers (RS PRO shim kit, RS Stock No.: 681-407 with a thickness of 310, 390, 490 and Fisherbrand™ Bonded Spacers, Product Code: 11807653 with thickness 570  $\mu\text{m}$ ) were fixed between two fluorosilane coated glass plates. To prepare the 2 mm support layer, glass plates coated with fluoro-silane having 1.0 mm attached spacers (Bio-rad Mini-PROTEAN® Spacer Plates, Catalog number: 1653311) were set up with a gap of 2 mm. To secure the mold and to avoid leakage of solution, the gap was sealed on three sides using autoclave tape. The precursor solution (~90°C) was poured through the open top until full. Very thin double network hydrogels < 200  $\mu\text{m}$  were prepared by adding a few drops of the precursor solution (~90 °C) onto one coated glass plate. Spacers (RS PRO shim kit, RS Stock No.: 681-407) were placed on either side of the drops and another salinized glass plate was placed on top. The space between the two plates was sealed on all four sides. The sealed assembly was allowed to cool to room temperature and UV treated for 60 min. (UVP model CL-1000, 365 nm, 8 Watt, 1000 mJ cm<sup>-2</sup>).

### 2.2 Characterization of the thickness of single layer hydrogels

Two methods of characterization were used for the hydrogel layers made using different spacer thicknesses (190  $\mu\text{m}$ , 310  $\mu\text{m}$ , 390  $\mu\text{m}$ , 490  $\mu\text{m}$  or 570  $\mu\text{m}$ )

- (1) vernier caliper (Duratool. D03196)
- (2) bright-field microscopy.

For bright-field microscopy, the gel layers were cut using a razor blade, and the cross-section was observed on a Leica microscope (DMC6200, HC PL FLUOTAR, 10x). The gels were then measured using Leica application suite X software (3.4.2.18368).

### 2.3 Fabrication multi-layered depth phantoms

Suspensions were made by adding 0.2 mg of signaling markers (polystyrene (PS) beads or fluorescent-silica (FS) beads or BaTiO<sub>3</sub>) in 200  $\mu$ L of ethanol in 1.5 ml Eppendorf tubes. PS suspensions were then sonicated for 30 min to avoid clustering and to achieve good dispersion. A SCS 6800 series spin coater was used to spin-coat (1000 rpm, 5 seconds) the suspensions of signaling markers onto 3 mm diameter circular glass coverslips using 5  $\mu$ L of suspension per coverslip. This was followed by drying coverslips in a desiccator for 30 minutes (under vacuum) or by simply leaving at room temperature for 12 hours.

A 6 mm x 6 mm section of double network hydrogel was made in contact with the coated coverslips on both sides, and the signaling markers transferred from the coverslip onto the gel. For multi-layered phantoms, coated hydrogel layers were stacked as required. Multi-layered phantoms were assembled on a 2 mm thick double network hydrogel support layer. The assembly was then inverted and with the 2 mm support layer on top, placed into a 4-well plate (Ibidi Cat.No: 80426). The multilayered assembly was gently pressed to ensure good contact with the surface and sealed in place using PDMS. For this purpose, a mixture of Vinyl terminated PDMS (SYLGARD™ 184 kit, Dow Corning) and curing agent (part of the kit) was mixed (9 g: 1 g), heated (80 °C, 3 min) in a hot oven and cooled to 25 °C before pouring into the wells containing the single or multi-layered phantoms. PDMS was added until the standards were completely immersed in the PDMS mixture. To ensure a good seal and avoid the presence of air bubbles in PDMS resin, the well plates were then placed in a glass desiccator under vacuum and allowed to cure for 24 hours at room temperature.

### 2.4 Single and Multiphoton imaging setup:

Single photon imaging was done using Zeiss Confocal Airscan and Zeiss Axiovert 200M, (Plan-Neofluar, 20X,  $\lambda_{ex}$  544 nm,  $\lambda_{em}$  570 nm). For multiphoton imaging including coherent anti-Stokes Raman scattering (CARS), second harmonic generation (SHG) and two-photon excitation fluorescence (2PEF), a custom-built, multimodal laser scanning microscope was used to acquire images (using ScanImage®,<sup>25</sup> Vidrio Technologies LLC) with). For CARS imaging, the Stokes beam was generated using a fiber laser (1031 nm, Emerald Engine, APE), and the pump beam was fundamental of optical parametric oscillator (OPO) (650–950 nm, Levante Emerald, APE GmbH). Same wavelengths were used for 2PEF and SHG excitation as well. All of the signals (CARS, SHG, 2PEF) were collected in epi-detection mode through the same objective and through the appropriate dichroic and band-pass filters, they were directed to three Hamamatsu photomultiplier tubes (PMTs).

## 3. RESULTS AND DISCUSSION

To overcome the major limitation of hydrogels i.e. stability and strength, two individual networks agarose and polyacrylamide were formed subsequently resulting in an interpenetrating network referred to as double network hydrogel. For this purpose, the mixture was prepared using one pot method<sup>5</sup> with the physically crosslinked agarose network forming first through a heat and cool cycle followed by ultraviolet (UV) curing resulting in the formation of the chemically crosslinked polyacrylamide network. This results in double network hydrogels that are very robust. The detailed synthesis procedure is described in the Experimental Section. Double network hydrogels can be easily molded into different shapes by selecting an appropriate mold during the casting stage (Figure 2 a, b). For the fabrication of depth standards, the mold used consisted of two glass plates separated by spacers of defined thicknesses (190  $\mu$ m, 310  $\mu$ m, 390  $\mu$ m, 490  $\mu$ m, 570  $\mu$ m or 2000  $\mu$ m). Gels were fabricated as thin layers ranging in size from 190  $\mu$ m to 2000  $\mu$ m. (Fig. 2)

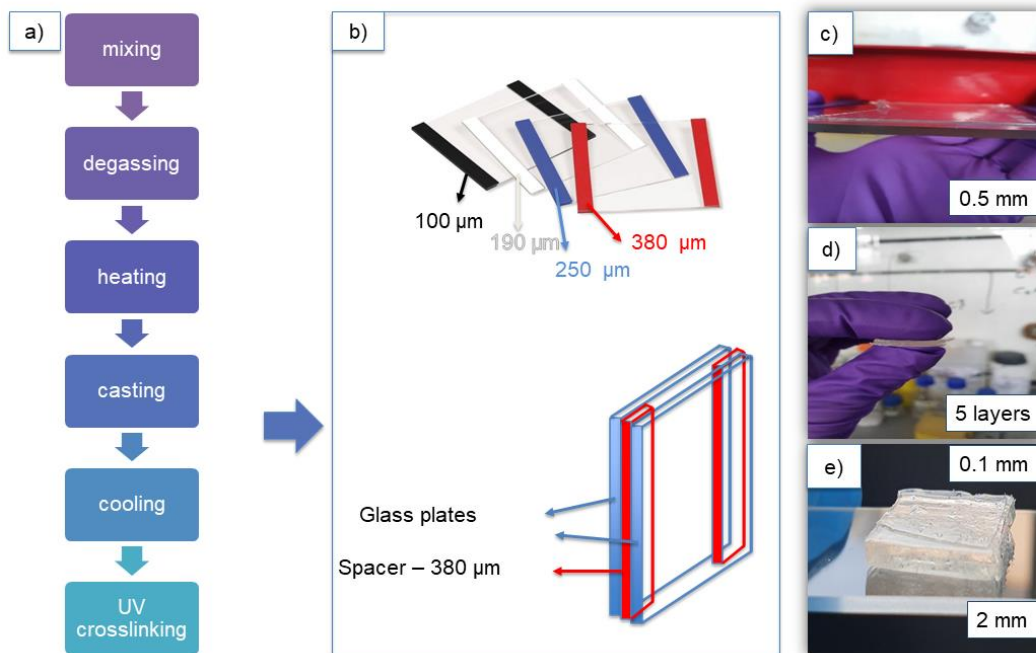


Figure 2: Synthesis of double network hydrogel in thin layers a) Flowchart showing the process for fabricating a double network hydrogel b) Mold and spacers used for the fabrication of gel in layers c) 500  $\mu\text{m}$  hydrogel layer b) Stack of 5 hydrogel layers e) Size range for double network hydrogel layers.

Single layers of double-network gels were measured axially using Vernier calipers and bright field microscopy (cross-section measurements of the gels). Both Vernier calipers and bright-field imaging measurements for the thickness of individual layers were consistent and agreed with spacer thickness (see Table 1 & Fig. 3)

Table 1: Vernier Caliper measurement of shim spacers and double network hydrogels.

	RS PRO Plastic Shim Kit ( $\mu\text{m}$ )	Measured hydrogel thickness. ( $\mu\text{m}$ )
a	190	$174 \pm 6$
b	310	$304 \pm 8$
c	390	$365 \pm 8$
d	490	$479 \pm 5$
e	570	$561 \pm 11$

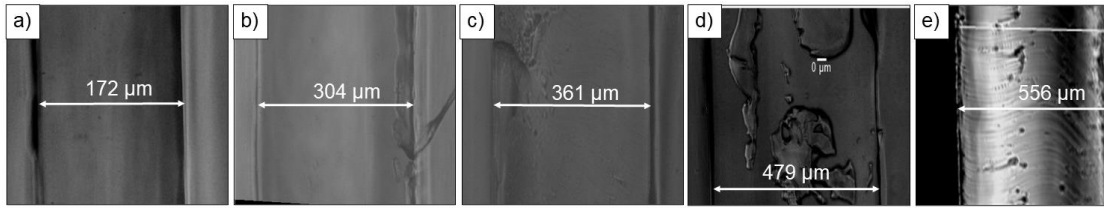


Figure 3: Thickness measured from the bright-field images of the double-network gels prepared using the plastic spacers with thicknesses of; a) 190  $\mu\text{m}$ , b) 310  $\mu\text{m}$ , c) 390  $\mu\text{m}$ , d) 490  $\mu\text{m}$ , and e) 570  $\mu\text{m}$ .

Sample for Single Photon Confocal imaging consisted of two layers of 190  $\mu\text{m}$  thicknesses sandwiched between three layers of signaling markers (FS beads) and capped on top with a 2000  $\mu\text{m}$  support layer. Confocal imaging was done using ZEISS Airyscan microscope ( $\lambda_{\text{ex}}$  430 nm). Two layers of the signaling markers could be imaged using this system but the second layer was barely visible. This can be due to the crowded first layer (Fig 2b) that makes it difficult for sufficient light to reach layer two of the signaling markers. Third position of signaling marker wasn't imaged on this system. The measured thickness of the gel was 141  $\mu\text{m}$  which is less than the expected thickness (190  $\mu\text{m}$ ) as indicated by the vernier caliper (Fig. 2). The possible reason for this difference in measured and actual value is discussed later in this section.

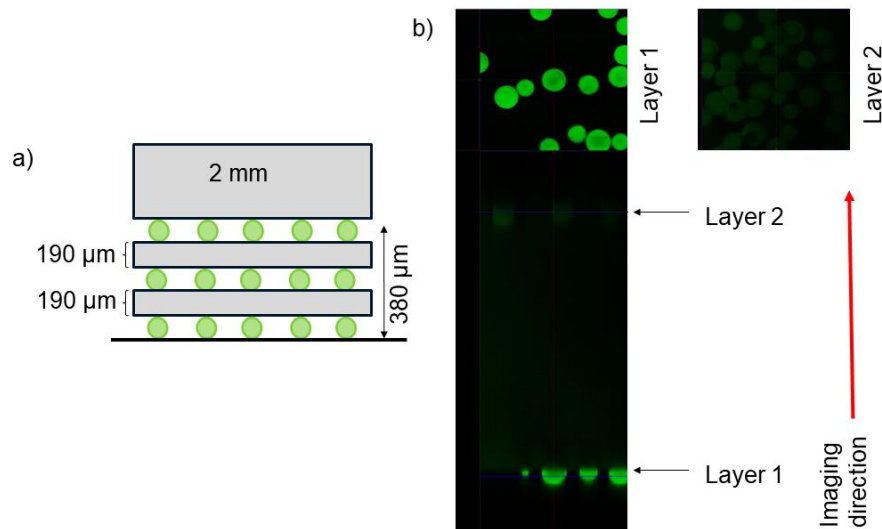


Figure 4: Single photon confocal microscopy a) Sample design: Two 190  $\mu\text{m}$  layers of hydrogels sandwiched between three layers of signaling markers (FS beads). A 2000  $\mu\text{m}$  support layer is placed on top of the bilayer sample. b) Orthogonal view showing images of two layers of signaling markers.

For the conventional single and multiphoton imaging modalities 1PEF, 2PEF, SHG and CARS depth standards were designed with 310  $\mu\text{m}$  hydrogel layers in between the layers of signaling markers (see Fig. 5 a, b, c, d). Signaling markers were specific to the imaging modality of interest e.g., fluorescent-silica (FS) beads for 1PEF and 2PEF, polystyrene (PS) beads for CARS and BaTiO<sub>3</sub> nanocrystals for SHG imaging.

The samples were imaged using ZEISS Axiovert 200M for single photon experiment using an excitation wavelength of 544 nm and emission was detected at 570 nm (Fig. 5e). A custom-built, multimodal laser scanning microscope (described in the Methods section) was used for the multiphoton imaging. Using two beams of 1031 nm and 797.2 nm wavelength respectively, FS beads were excited via degenerate two-photon excitation. Nondegenerate two photon excitation of their combination, as verified by the partial delay dependence of the signal, was also collected in the

spectral range between 530 to 570 nm (Fig. 5f). For CARS imaging the C–H stretching mode of polystyrene beads at 2845 cm<sup>-1</sup> was used, by tuning the OPO at 797.2 nm and collecting the anti-Stokes at 650 nm (Fig 5g). Finally, SHG imaging for imaging BaTiO<sub>3</sub> crystals was done using the OPO beam and collecting the corresponding signal around 400 nm (Fig. 5h). For acquiring the images of signaling markers, the beads and crystals were imaged at position where maximum contrast could be seen by eyes and the diameter of beads could be determined.

In samples constructed with the 310 μm hydrogel layers, 6 layers of signaling markers were imaged using 1PEF and 2PEF which reached depths of 1033 and 1046 μm. By comparison, using SHG and CARS imaging, only 5 layers of depth standards were imaged, reaching depths of 835 μm and 814 μm respectively. (Fig. 5 e, f, g, h) (this limitation in imaging depth was due to the working distance of objective which was 1000 μm). However, the values observed in both single and multi-photon imaging systems were different than the expected values of overall depth calculated using the vernier caliper measurements of individual layers. This difference in depths is expected due to difference in refractive index of the two media (hydrogel and air) resulting in measured depths that are either shorter or longer than the actual depth.<sup>6</sup> For imaging depths >500 μm, the incident laser power needed to be increased to generate sufficient signal.

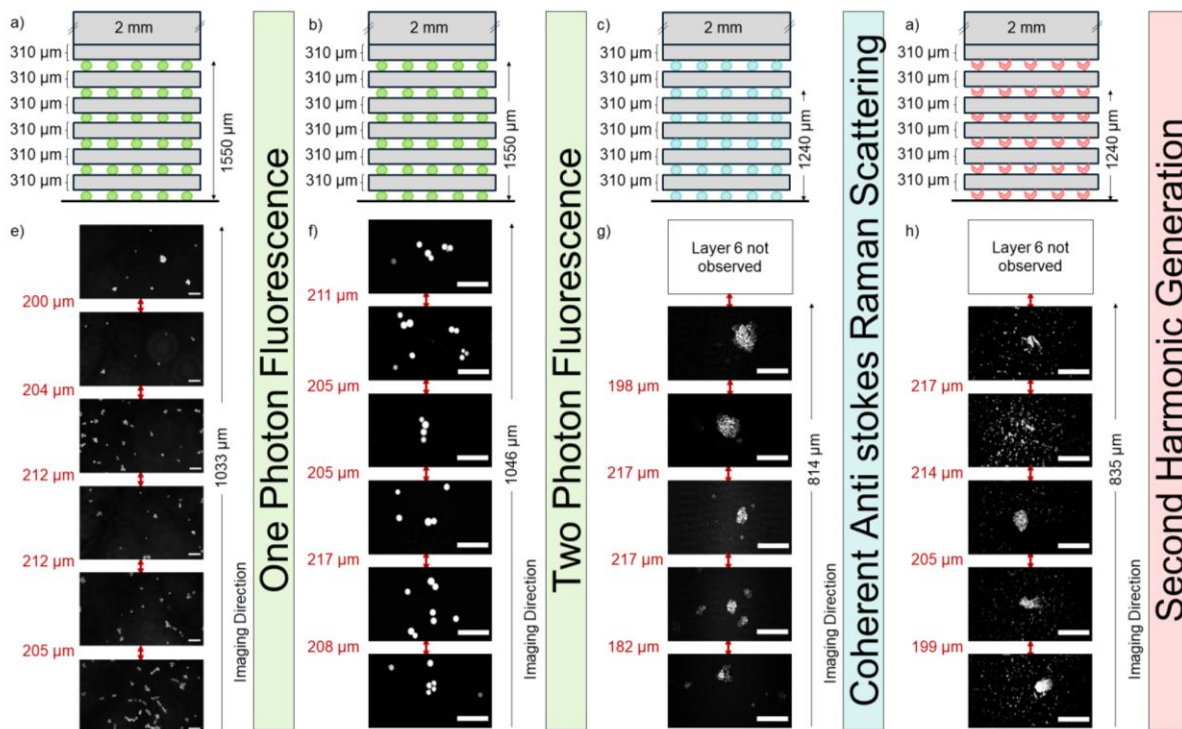


Figure 5: Analysis of depth standard on multimodal imaging systems. a, b, c, d: Depth standards incorporating fluorescent beads (Green), Polystyrene beads (Blue), and BaTiO<sub>3</sub> (Red) imaged via One photon fluorescence, Two photon fluorescence, Coherent anti-Stokes Raman scattering, and Second harmonic generation, respectively. Each depth standard had 6 layers of signaling markers (BaTiO<sub>3</sub>/ fluorescence beads/or polystyrene beads) sandwiching 5 layers of hydrogels of defined thicknesses (310 μm) giving an overall height of 1550 μm. e, f, g, h: 1PEF, 2PEF, SHG and CARS imaging up to depths of 1033 μm, 1046 μm, 835 μm, and 814 μm. The microscopy images represent the marker layers and the distances between each layer is given in red. The scale bar represents 50 μm.

#### 4. CONCLUSIONS

We designed and fabricated robust standards that can be stored at room temperature and utilized for on spot verification and testing of different optical systems. The phantoms proved robust tools for imaging depth analysis of various imaging modalities including 1PEF, 2PEF, SHG and CARS allowing imaging depths of up to 1 mm. Our depth standards have

the potential to be used for calibration of axial positioning and movement of microscope systems. These standards also have potential to be used with adaptive optics for correction of optical aberrations at depth in order to facilitate the process of deep tissue imaging.

## REFERENCES

- [1] Sarder, P., Yazdanfar, S., Akers, W. J., Tang, R., Sudlow, G. P., Egbulefu, C. and Achilefu, S., "All-near-infrared multiphoton microscopy interrogates intact tissues at deeper imaging depths than conventional single- and two-photon near-infrared excitation microscopes," *Journal of biomedical optics*, 18(10), 106012-106012 (2013).
- [2] Corbett, A. D., Shaw, M., Yacoot, A., Jefferson, A., Schermelleh, L., Wilson, T., Booth, M. and Salter, P. S., "Microscope calibration using laser written fluorescence," *Optics express*, 26(17), 21887-21899 (2018).
- [3] Yim, W., Zhou, J., Sasi, L., Zhao, J., Yeung, J., Cheng, Y., Jin, Z., Johnson, W., Xu, M., Palma-Chavez, J., Fu, L., Qi, B., Retout, M., Shah, N. J., Bae, J. and Jokerst, J. V., "3D-bioprinted Phantom with Human Skin Phototypes for Biomedical Optics," *Adv. Mater.*, 35, 2206385 (2022).
- [4] Fales, A. M., Strobbia, P., Vo-Dinh, T., Ilev, I. K. and Pfefer, T. J., "3D-printed phantoms for characterizing SERS nanoparticle detectability in turbid media," *Analyst*, 145(18), 6045-6053 (2020).
- [5] Chen, Q., Zhu, L., Zhao, C., Wang, Q. and Zheng, J., "A Robust, One-Pot Synthesis of Highly Mechanical and Recoverable Double Network Hydrogels Using Thermoreversible Sol-Gel Polysaccharide," *Adv. Mater.*, 25(30), 4171-4176 (2013).
- [6] Haseeb, F., Bourdakos, K. N., Forsyth, E., Setchfield, K., Gorman, A., Venkateswaran, S., Wright, A. J., Mahajan, S. and Bradley, M. "Development of hydrogel-based standards and phantoms for non-linear imaging at depth," *Journal of Biomedical Optics*, 28(12), 126007-126007 (2023).